Epilepsy & Behavior 71 (2017) 193–206

Contents lists available at ScienceDirect

Epilepsy & Behavior

journal homepage: www.elsevier.com/locate/yebeh

Morphofunctional alterations in the olivocochlear efferent system of the genetic audiogenic seizure-prone hamster GASH:Sal

David Sánchez-Benito [a,b,c], Ricardo Gómez-Nieto [a,b,c], Sonia Hernández-Noriega [a,b], Adriana Andrade Batista Murashima [d], José Antonio Cortes de Oliveira [e], Norberto Garcia-Cairasco [e], Dolores E. López [a,b,c,*], Miguel Angelo Hyppolito [d]

[a] Institute of Neuroscience of Castilla y León (INCYL), University of Salamanca, Salamanca, Spain
[b] Institute of Biomedical Research of Salamanca (IBSAL), University of Salamanca, Salamanca, Spain
[c] Department of Cell Biology and Pathology, Faculty of Medicine, University of Salamanca, Salamanca, Spain
[d] Laboratory of Neurobiology of Hearing, Ribeirão Preto Medical School, University of São Paulo, São Paulo, Brazil
[e] Neurophysiology and Experimental Neuroethology Laboratory, Ribeirão Preto Medical School, University of São Paulo, São Paulo, Brazil

ARTICLE INFO

Article history:
Received 9 December 2015
Revised 13 May 2016
Accepted 31 May 2016
Available online 1 August 2016

Keywords:
Animal models of epilepsy
Reflex seizures
Distortion-product otoacoustic emission (DPOAE)
Hair cell
Olivocochlear neurons
Pathogenesis of epilepsy
Scanning electron microscopy

ABSTRACT

The genetic audiogenic seizure hamster (GASH:Sal) is a model of a form of reflex epilepsy that is manifested as generalized tonic–clonic seizures induced by external acoustic stimulation. The morphofunctional alterations in the auditory system of the GASH:Sal that may contribute to seizure susceptibility have not been thoroughly determined. In this study, we analyzed the olivocochlear efferent system of the GASH:Sal from the organ of Corti, including outer and inner hair cells, to the olivocochlear neurons, including shell, lateral, and medial olivocochlear (LOC and MOC) neurons that innervate the cochlear receptor. To achieve this, we carried out a multi-technical approach that combined auditory hearing screenings, scanning electron microscopy, morphometric analysis of labeled LOC and MOC neurons after unilateral Fluoro-Gold injections into the cochlea, and 3D reconstruction of the lateral superior olive (LSO). Our results showed that the GASH:Sal exhibited higher auditory brain response (ABR) thresholds than their controls, as well as absence of distortion-product of otoacoustic emissions (DPOAEs) in a wide range of frequencies. The ABR and DPOAE results also showed differences between the left and right ears, indicating asymmetrical hearing alterations in the GASH:Sal. These alterations in the peripheral auditory activity correlated with morphological alterations. At the cochlear level, the scanning electron microscopy analysis showed marked distortions of the stereocilia from basal to apical cochlear turns in the GASH:Sal, which were not observed in the control hamsters. At the brainstem level, MOC, LOC, and shell neurons had reduced soma areas compared with control animals. This LOC neuron shrinkage contributed to reduction in the LSO volume of the GASH:Sal as shown in the 3D reconstruction analysis. Our study demonstrated that the morphofunctional alterations of the olivocochlear efferent system are innate components of the GASH:Sal, which might contribute to their susceptibility to audiogenic seizures.

This article is part of a Special Issue entitled "Genetic and Reflex Epilepsies, Audiogenic Seizures and Strains: From Experimental Models to the Clinic".

© 2016 Elsevier Inc. All rights reserved.

1. Introduction

The genetic audiogenic seizure hamster (GASH:Sal), in which exposure to intense acoustic stimulation induces generalized convulsive audiogenic seizures, is a strain of Syrian hamster inbred at the University of Salamanca [1]. Recent studies have supported the GASH:Sal as a promising animal model to study the development of epileptic seizures [2–4] and the characterization of antiepileptic drugs [5,6]. Functional, electrophysiological, and structural characterization of the auditory pathways in the GASH:Sal might be a further step towards understanding the pathophysiological mechanisms involved in different types of seizures including focal and generalized tonic–clonic seizures. In fact, several studies reported that the hyperactivity of an important midbrain auditory structure, the inferior colliculus (IC), is implicated in the initiation and propagation of audiogenic seizures [7].

Several audiogenic seizure-susceptible strains have been genetically selected worldwide [8,9]. The GASH:Sal was originated at the University

* Corresponding author at: Institute for Neuroscience of Castilla y León (INCyL), Laboratory 12, C/ Pintor Fenando Gallego 1., 37007 Salamanca, Spain. Tel.: +34 923294400x1868.
E-mail address: lopezde@usal.es (D.E. López).

http://dx.doi.org/10.1016/j.yebeh.2016.05.040
1525-5050/© 2016 Elsevier Inc. All rights reserved.

of Salamanca [1] and exhibits epileptic seizures in response to sounds [3,4]. After acoustic stimulation, the seizure appears within seconds and lasts for approximately 5 min, following a sequence of behavioral phases: wild running, tonic–clonic seizures, and a comatose postictal phase with subsequent recovery. The GASH:Sal hamsters exhibit their maximum susceptibility to seizures from 1 to 4 months of age, but this condition gradually disappears around the age of 1 year, showing the running phase without the convulsive phase [4,5].

Experimental models of epilepsy are necessary for understanding the neural substrates and neurochemical mechanisms involved in epileptogenesis, as well as for determining the mechanisms of drug action in clinical practice and selection of new anticonvulsant agents. Each model has specific characteristics regarding motor expression, electroencephalography, and response to different antiepileptic drugs. The rodent models (usually rats and mice) of electrically [10] and acoustically induced acute and chronic seizures have been associated with partial and generalized tonic–clonic seizures, with selective involvement of brainstem and limbic structures [11]. The IC, deep layers of superior colliculus, reticular formation, substantia nigra pars reticulata, and periaqueductal gray matter are implicated in the pathophysiological aspects of audiogenic seizures [11–13].

The possible morphofunctional alterations in the auditory system of the GASH:Sal, including the superior olivary complex (SOC) and the cochlear receptor, which might be involved in the expression of their audiogenic seizures, have not been thoroughly studied. The SOC, a collection of brainstem nuclei that participate in multiple aspects of hearing, contains the source of the olivocochlear system that innervates the cochlea. In mammals, the olivocochlear neurons form a dense bundle of fibers which projects bilaterally from the SOC to the organ of Corti. This olivocochlear bundle is divided into two efferent systems based on the cell bodies' site of origin and the projection pattern: 1) the lateral superior olive (LSO), a distinct group of neurons located in the lateral part of the SOC that forms the lateral olivocochlear (LOC) system, and 2) the ventral nucleus of the trapezoid body (VNTB), a diffuse and heterogeneous group of neurons located ventrally within the complex that forms the medial olivocochlear (MOC) system. Lateral olivocochlear neurons send unmyelinated axons to project beneath the inner hair cells (IHCs) of the cochlea, with a clear ipsilateral preference. On the contrary, MOC neurons send their myelinated axons to innervate the outer hair cells (OHCs) of the cochlea with a contralateral preference [14]. Afferent inputs to LOC neurons originate almost exclusively from the ipsilateral cochlear nucleus. Those to MOC neurons are somewhat more complex and include predominantly contralateral projections from the cochlear nuclei, as well as descending fibers from the IC and the auditory cortex [15,16].

The inputs descending from higher levels are thought to underlie the possible involvement of the MOC system in selective attention [17–20]. In addition to these classically defined LOC and MOC neurons, neuronal tract-tracing studies revealed a third class of olivocochlear neurons, called “shell neurons”, which surround the LSO [21]. Lateral olivocochlear neurons have round spherical cell bodies that are located within the LSO, and hence, they are referred to as intrinsic LOC neurons. In contrast, shell neurons are referred to as extrinsic because they are located surrounding the LSO. Shell neurons project mainly to the ipsilateral cochlea, they are larger than intrinsic LOC neurons, and their somata are morphologically similar to MOC neurons, which have large multipolar cell bodies. Lateral olivocochlear neurons are tonotopically organized within the LSO with high-to-low frequencies represented from medial to lateral. Although this organization within the nucleus is not that clear for MOC neurons, their afferent and efferent projections are organized in a tonotopic fashion. The functional role of the MOC and LOC systems is, in general, to reflexively modulate the sensitivity of receptor mechanisms operating in relation to each type of hair cell within the organ of Corti [22–25]. Evidence of the action of the medial olivocochlear efferent system has been obtained by the suppression of the so-called distortion-product of otoacoustic emissions (DPOAEs), following acoustic stimulation.

Therefore, hearing evaluation using DPOAEs and auditory brainstem responses (ABRs) provides valuable information on functional, morphological, and electrophysiological aspects of the auditory system and particularly on the olivocochlear efferent pathway and the cochlear status, giving information about hair cell function. In fact, DPOAEs measure the feedback of biomechanic energy to the contraction of the outer hair cells [26]. The ABR measures the bioelectrical phenomena triggered by the sound stimulus through the auditory brainstem. This electrical activity can be filtered and captured by surface electrodes and is represented by 5 to 7 waves (I, II, III, IV, V, VI, and VII), each one of them referring to a specific location of the central auditory pathway. In rodents, the elicited waveform response has the following correlation: wave I, auditory nerve; wave II, cochlear nuclei; wave III, superior olivary complex; wave IV, lateral lemniscus and IC; and wave V, medial geniculate body and thalamocortical auditory radiation. The present study aimed to determine whether the olivocochlear system of the GASH:Sal has functional and morphological alterations that might explain its susceptibility to audiogenic seizures. Thus, functional assessment of the olivocochlear system was carried out using DPOAE and ABR tests in the GASH:Sal. Furthermore, in order to assess possible morphological alterations, we performed a morphometric analysis of MOC, LOC, and shell neurons as well as a 3D reconstruction analysis of the LSO. Since olivocochlear alterations might lead to cilia malfunctioning, we further studied the organ of Corti by employing the scanning electron microscopy in order to determine any derangement or distortion of cilia. All these morphological studies in the GASH:Sal were compared to control animals and correlated to the electrophysiological examinations. Our data represent the first link of functional and morphological alterations in the auditory system of the GASH:Sal hamsters that might contribute to their audiogenic seizure susceptibility.

2. Material and methods

2.1. Experimental animals

In total, 9 control hamsters (*Mesocricetus auratus*) from Charles River Labs (Barcelona, Spain) and 16 hamsters of the GASH:Sal strain from the animal's facility of the University of Salamanca (Salamanca, Spain), 4 months of age, were used in this study. All the GASH:Sal hamsters were naïve without receiving any acoustic stimulation to trigger audiogenic seizures. The experiments were conducted in compliance with the guidelines for the use and care of laboratory animals of the European Communities Council Directive (2010/63/EU), with the current Spanish legislation (RD 1201/05), and with those established by the Institutional Bioethics Committee. All efforts were made to minimize the number of animals and their suffering. The animals were maintained under normal conditions of lighting (12-h light/dark cycle) and constant temperature with ad libitum access to food and water.

2.2. DPOAE and ABR tests

For the functional and electrophysiological auditory assessment, 8 GASH:Sal and 3 control hamsters were evaluated for DPOAE and ABR tests under anesthesia with ketamine hydrochloride (40 mg/kg) and xylazine (10 mg/kg) via intramuscular administration. Studies were performed with the Smart EP-DPOAE equipment manufactured by Intelligent Hearing Systems (Miami, FL, USA) and calibrated by the manufacturer. Analysis of DPOAE was performed following the relationship of frequencies of 2f1–f2 with f1:f2 = 1.22, two points per octave resolution (DPGRAM). The DPOAEs were 55-dB SPL less intense than the stimulus.

The DPGRAM provides information about function of the cochlear outer hair cells that were responsible for the analyzed frequencies. For evaluation of the auditory threshold, the ABR test was performed.

Surface electrodes were positioned as follows: a positive electrode on the cranial vertex, two negative electrodes in the posterior portion of the pinna, and a reference electrode (ground) on the forehead, between the orbits. These electrodes were placed with interposition of electrolytic paste, for better conductivity of electrical signal and reduction of artifacts. For sound stimulation, inserted headphones were placed in the external auditory canal. The stimulus used was the alternated click, with 27.7 stimuli per second and a duration of 0.1 ms. Fundamental frequency was 2000–4000 Hz, using the intensity of 90-dB nHL. The signal picked up by electrodes was pass filtered — high and low of 150 and 3000 Hz, respectively. The filtered and amplified signal was the average of 1024 ABR recordings, with a window of 12 ms. The final result was provided in the form of waves of electric potential. The research of the auditory threshold was performed by means of sound stimulus which was decreased by 10 dB until the approximate threshold. The threshold was considered as the lowest intensity in which the first wave of auditory potential was obtained. For the ABR tests, we used Smart EP—Intelligent Hearing Systems (Miami, FL, USA), calibrated by the manufacturer. The latency of each ABR component was measured at an intensity of 90 dB.

2.3. Scanning electron microscopy study

For the scanning electron microscopy study of the cochlear hair cells, 1 control and 3 GASH:Sal hamsters were used. The tissue was obtained by perfusion of each animal after anesthesia with sodium thiopental (Abbott) (69 mg/kg). Animals were perfused transcardially with 0.1-M phosphate buffer solution, followed by 4% paraformaldehyde and 0.1% glutaraldehyde in 0.1 M of phosphate buffer (pH = 7.4) using a speed-controlled pump perfusion Masterflex® (Paste, Parmer). Then, a craniotomy was performed to quickly remove the brain and the tympanic bulla. The bulla was opened, and the cochlea was dissected under the microscope and perfused in 4% paraformaldehyde solution and subsequently maintained in the same fixative solution for 4 h.

Cochleae were processed for scanning electron microscopy, washed three times for 5 min with 0.1 M phosphate buffer (pH = 7.4). After these procedures, cochleae were fixed in 1% osmium tetroxide solution in 0.1-M phosphate buffer (pH = 7.4), for 2 h at 4 °C, washed with phosphate buffer solution 0.1-M (pH = 7.4), and dehydrated at room temperature in graded concentrations of ethanol (50%, 70%, 90%, and 95% — once for 10 min at each concentration) and absolute ethanol three times for 15 min. Completed dehydration was performed following the drying method of critical point in CO_2, using the equipment BAL-TEC CPD 030® (Critical Point Dryers), in which after successive baths in liquid CO_2 at 4 °C, the ethanol was removed. Then, the material was subjected to an increase in temperature to 40 °C in order to pass CO_2 from liquid to gaseous state. The material was fixed in a metal support, being coated in a vacuum chamber BAL-TEC SCD 050 with vapors of gold. After this tissue preparation procedure, the cochleae were electrically conductive. The observation and analysis of the cochlear hair cells were carried out with an Electron Microscope JEOL SCANNING MICROSCOPE — JSM 5200.

2.4. Injection of Fluoro-Gold

For the morphological study of the olivocochlear neurons, 3 control and 3 GASH:Sal hamsters received unilateral injections of the retrograde tracer Fluoro-Gold® (FG — Fluorochrome, Denver, CO, USA), diluted in 4% in saline solution, into the left cochlea. Animals were prepared under deep anesthesia with ketamine (200 mg/kg) and xylazine (10 mg/kg), and when necessary, an anesthetic complementation with 1/5 of the initial dose was injected during the surgery. In addition, local anesthetic (2% lidocaine with epinephrine 1:200,000) was administered before surgery. After a skin incision and removal of adipose tissue in the postauricular region, the tympanic bulla was exposed. Then, the bulla was opened with a diamond drill, and the round window of the cochlea was visualized. The FG was injected by pressure into the cochlea through the round window using a micropipette of glass with a diameter of 50–60 μm. After the injection, the bulla was sealed with bone wax, and the incision was sutured. Animals recovered from surgery, following a postinjection survival time of 10 days, and immediately after that, they were processed for histology. Under deep anesthesia with sodium pentobarbital, hamsters were perfused transcardially with a Ringer's solution (37 °C, pH 6.9), followed by 4% paraformaldehyde. The brains were removed and cryoprotected for 48–72 h at 4 °C in a solution containing 30% sucrose. Serial coronal brainstem sections of 40-μm thickness were obtained in a freezing microtome. The FG was visualized following the immunohistochemical procedure described by Gómez-Nieto et al. [27]. All sections were incubated with a rabbit anti-FG antibody (dilution 1:2000), followed by a goat biotinylated secondary antibody anti-rabbit (dilution 1:200). Then, the sections were incubated in the avidin–biotin–peroxidase complex, developed for peroxidase reaction, mounted on slides, dehydrated in ethanol, and coverslipped as described by Gómez-Nieto et al. [27].

2.5. 3D reconstruction

Four animals, 2 control and 2 GASH:Sal hamsters, were employed to generate 3D reconstructions of the LSO using Neurolucida (version 10) and NeuroExplorer (version 3) software applications from MicroBrightField Bioscience, (Williston, VT, USA) following the procedure described elsewhere [28]. After perfusion of the animal, the brain was collected, and a hole was made by the passage of a surgical needle throughout the rostrocaudal plane of the left brainstem, and serial brain sections were obtained as described above. Then, alternate serial sections were processed for immunohistochemical visualization of the calcium-binding protein, calbindin D-28k (CaBP), using an identical procedure to the one used by Gómez-Nieto et al. [27]. For each brain, all sections were mounted on slides, and alternate series without immunohistochemistry for CaBP were counterstained with cresyl violet to highlight cytoarchitectonic divisions; the other sections processed for CaBP immunohistochemistry were dehydrated in ethanol and coverslipped. The outline of CaBP and cresyl violet-stained coronal sections was viewed with the 5× objective lens of a Leica DMRB microscope and was drawn on the computer screen. Successive sections were aligned via rotation and translation of the drawing with the help of four reference points. The hole, created by the needle, was used for setting one of these reference points, and the other three were set using different anatomical landmarks as the edges of adjacent sections. All these structures were superimposed and matched in the two successive sections to achieve accurate alignment. After that, the contours of the LSO were manually traced using a 20× objective lens. The contours of the brainstem and the LSO were digitized with Neurolucida and metrically and topologically analyzed with NeuroExplorer. Images and movie documents from the 3D renderings were obtained using Neurolucida software.

2.6. Imaging and data analysis

The histological sections processed for light microscopy were examined using a Leica microscope DMLB, coupled to a drawing tube and a digital camera to obtain the images. Low magnification images were taken with the 4× and 10× objective lens, and high magnification images were taken with a 40× objective lens. Drawing schemes of brainstem sections were carried out using the camera Lucida and digitalized with the Canvas software (version 14 Build 1618, ACD Systems of America, Inc.). The morphometric analysis of labeled olivocochlear neurons was carried out with ImageJ (version 1.42; Rasband, N.S., National Institutes of Health, Bethesda, Maryland, USA; http://rsb.info.nih.gov/ij). For the scanning electron microscopy study, images of the basal, medial, and apical cochlear turns were obtained at a magnification that ranged from 2000× to 3500×. All representative images shown in the figures were processed by minor modifications with regard to brightness

and contrast using ImageJ, and the final figures were composed with Canvas 14.

Statistical analysis of the morphometric features such as area, perimeter, and roundness of labeled olivocochlear neurons, as well as the volume and area of the 3D reconstruction, was performed using the SPSS software, version 18.0 (SPSS Inc., Chicago, IL, USA). For each of the morphometric parameters in the labeled neurons, one factor analysis of variance test and post hoc analysis with Fisher's PLSD and Sheffe's test were applied. We considered six groups for the statistical comparisons between the control and GASH:Sal hamsters: ipsilateral and contralateral intrinsic LOC neurons, ipsilateral and contralateral shell neurons, and ipsilateral and contralateral MOC neurons. All values were expressed as the mean ± standard error of the mean.

3. Results

3.1. ABR and DPOAE evaluations in the GASH:Sal

We performed a hearing screening of the GASH:Sal at 4 months of age by combining the two existing hearing tests: (1) the ABR test and

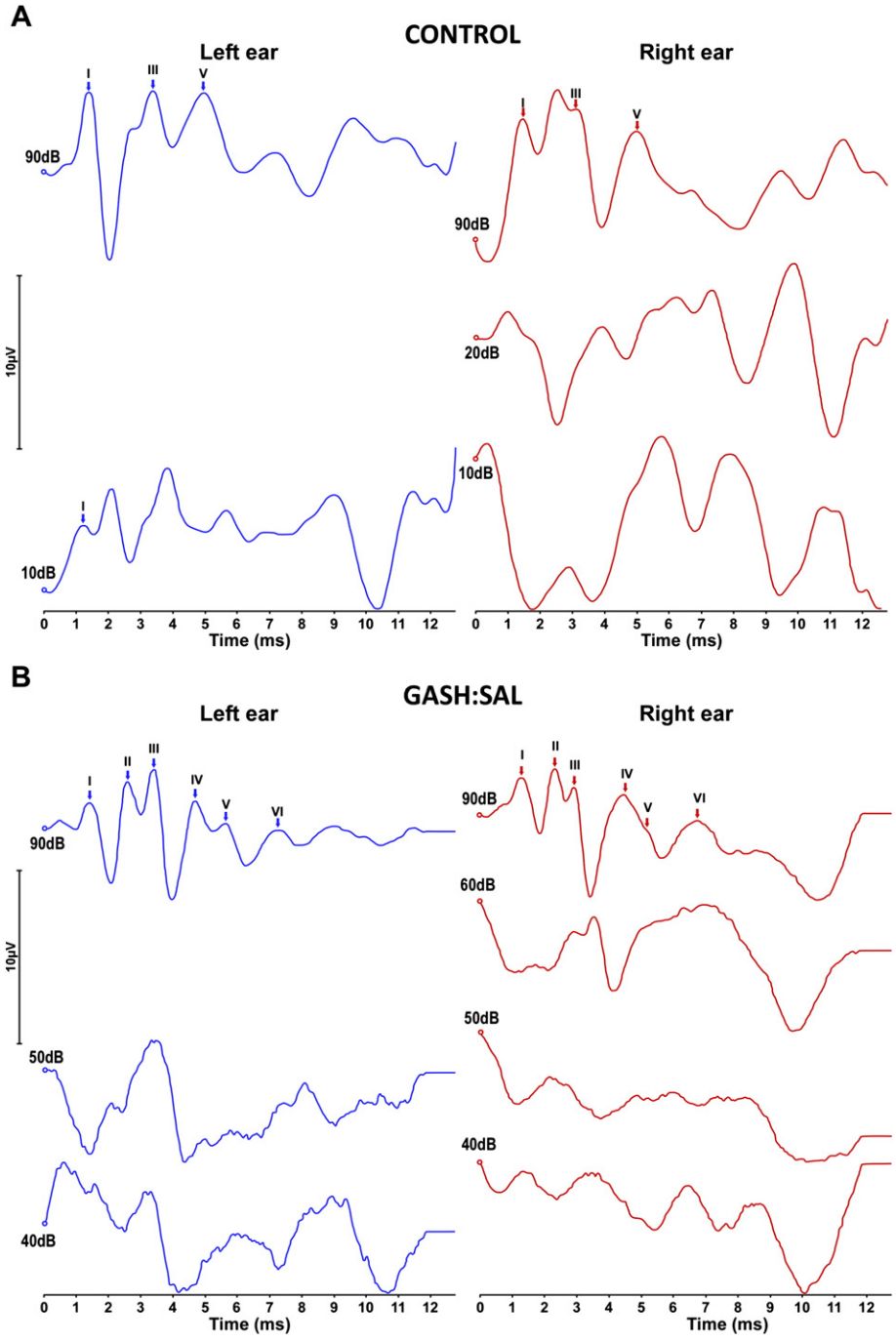

Fig. 1. Auditory brain response (ABR) evaluations in the control and GASH:Sal hamsters. A. Plots show ABR waveforms (amplitude in μV) obtained from one control hamster after click stimulation on the left (in blue) and right (in red) ears. Notice that the ABR thresholds are 20 dB. B. Plots show ABRs (amplitude in μV) obtained from one GASH:Sal hamster after click stimulation on the left (in blue) and right (in red) ears. Notice that thresholds of ABRs are 50 dB and 60 dB for the left and right ears, respectively. The plots showed representative ABR recordings at the smallest intensity of clicks which evoked visually detectable responses (ABR threshold) and the maximum intensity (90 dB), in which ABR waveforms were clearly visible. All responses displayed in the graphs were double-traced to confirm reproducibility (not shown in this figure).

(2) the DPOAE test. The ABR test showed that the lowest intensity in which the wave responses could be detected was 50 dB and 60 dB at 2–4 kHz for the left and right ears, respectively (Fig. 1). The identification of more appropriate latency–amplitude wave responses was observed at an intensity of 90 dB (Fig. 1). On the contrary, the control hamsters exhibited ABR thresholds of 20 dB, and hence, the ABR thresholds in the GASH:Sal were elevated approximately 30–40 dB more than in controls (see Fig. 1A–B for comparison).

A comparison of the ABR results between the right and left ears of the GASH:Sal showed an increase of approximately 0.5 to 1.3 ms in the latency of the left ear for each of the wave responses (Fig. 2). The latencies of the waves III, IV, and V were significantly higher for the left than for the right ear of the GASH:Sal. Such differences were not observed in the control hamster (see Fig. 2A–C for comparison). We further analyzed the ABR interpeak latencies of the wave's responses (Fig. 2). Thus, the GASH:Sal showed significantly higher interpeak latencies between the waves III and V as well as the waves I and V for the left than for the right ear stimulation (p value ≤ 0.05). By contrast, there were no statistically significant differences in the ABR latencies when comparing the left and right ears of the control hamsters (see Fig. 2B–D for comparison).

The DPOAE tests in the GASH:Sal showed that DPOAEs were absent in the low–middle frequency range from 500 to 6000 Hz in both ears. However, DPOAEs were observed at frequencies above 6000 Hz (Fig. 3). The DPOAEs at a frequency of 8000 Hz exhibited higher amplitude for the left than for the right ear, this difference being statistically significant (p value ≤ 0.001) (Fig. 3). On the contrary, the control hamsters exhibited normal DPOAEs for both ears at all frequencies (for comparison, see Fig. 3A–B and C–D).

3.2. Scanning electron microcopy study of the cochlear hair cells

The higher thresholds shown in the ABR tests of the GASH:Sal as well as the differences in the latency of ABRs and DPOAEs between the left and right ears led us to study the cochlear hair cells of the GASH:Sal with the scanning electron microscopy. Our results showed that the cochlea of control hamsters exhibited the ordered cellular mosaic pattern made of the apical domains of hair cells, as well as the supporting cells in the organ of Corti. The three rows of OHCs were separated from the single row of IHCs by the inner pillar cells (Fig. 4A). The OHCs and IHCs were characterized by tufts of stereocilia protruding from their apices. Stereocilia were observed as cylindrical protrusions morphologically similar to large microvilli. The stereocilia of IHCs formed straight or slightly curved bundles, while the stereocilia of the OHCs exhibited a V-shaped pattern (Fig. 4A). The organ of Corti of the GASH:Sal revealed a similar distribution of OHCs and IHCs than the one observed in the control hamster. The three rows of OHCs and a single row of IHCs were also present in the GASH:Sal, showing no differences in the number of cochlear hair cells between these two animal groups (Fig. 4). However, the stereociliary organization of the cochlear hair cells in the GASH:Sal was markedly different compared with that in the control hamsters. Such alterations in the stereocilia pattern were more noticeable in the basal turn of the cochlea. The majority of OHCs and IHCs showed disorganization of the tufts of stereocilia and loss of their links (Fig. 4B). Occasionally, these stereocilia appeared to be shortened and collapsed. In the medial turn of the cochlea, stereociliary distortion and disarrangement were frequently noticed in the OHCs, especially in the first row of OHCs, as well as in the IHCs (Fig. 4C). The apical turn of the cochlea in the GASH:Sal was the least altered of the three cochlear

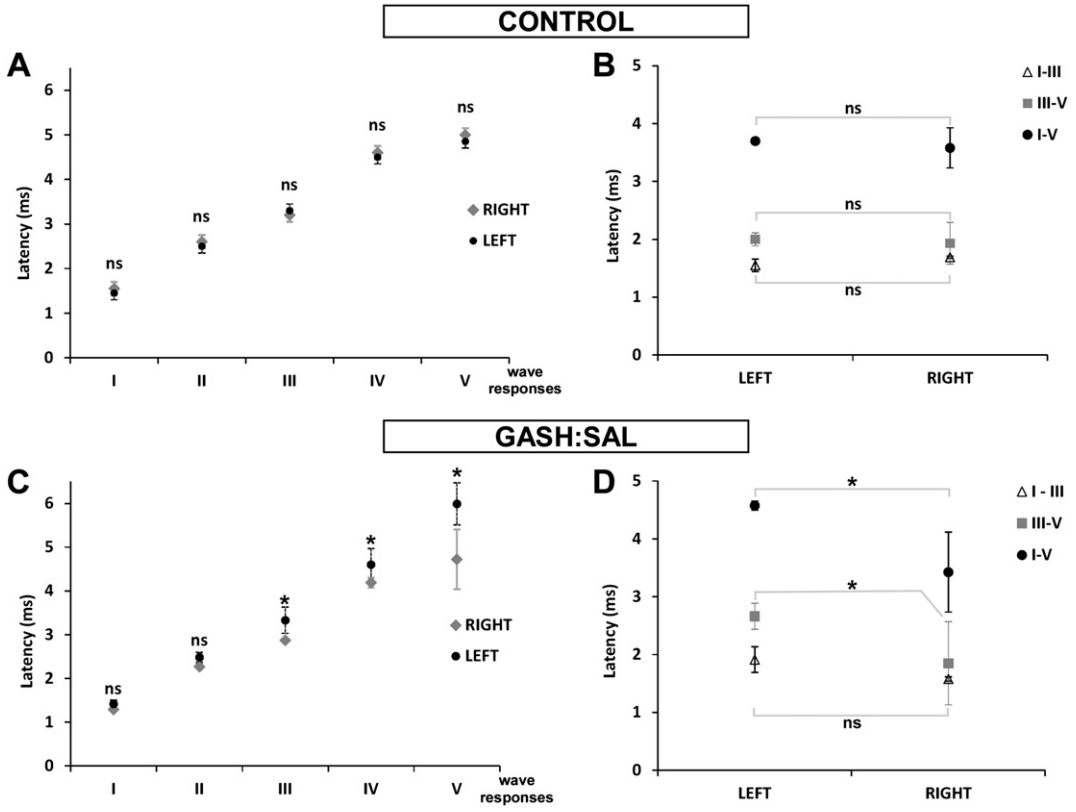

Fig. 2. Latencies of auditory brain responses (ABRs) in the control and GASH:Sal hamsters. A. Plot shows latencies for each waveform responses (I, II, III, IV, and V) in the left and right ears of the control hamsters. B. Plot shows interpeak latencies in the left and right ears of control hamsters. Notice that there were no significant differences between the left and right ears. C. Plot displays latencies for each waveform responses in the GASH:Sal. Notice significantly shorter latencies in the waves III, IV, and V for the right-ear stimulation. D. ABR interpeak latencies in the GASH:Sal hamsters, showing longer latency intervals for the left-ear stimulation. "*" = p value ≤ 0.05. ns = nonsignificant.

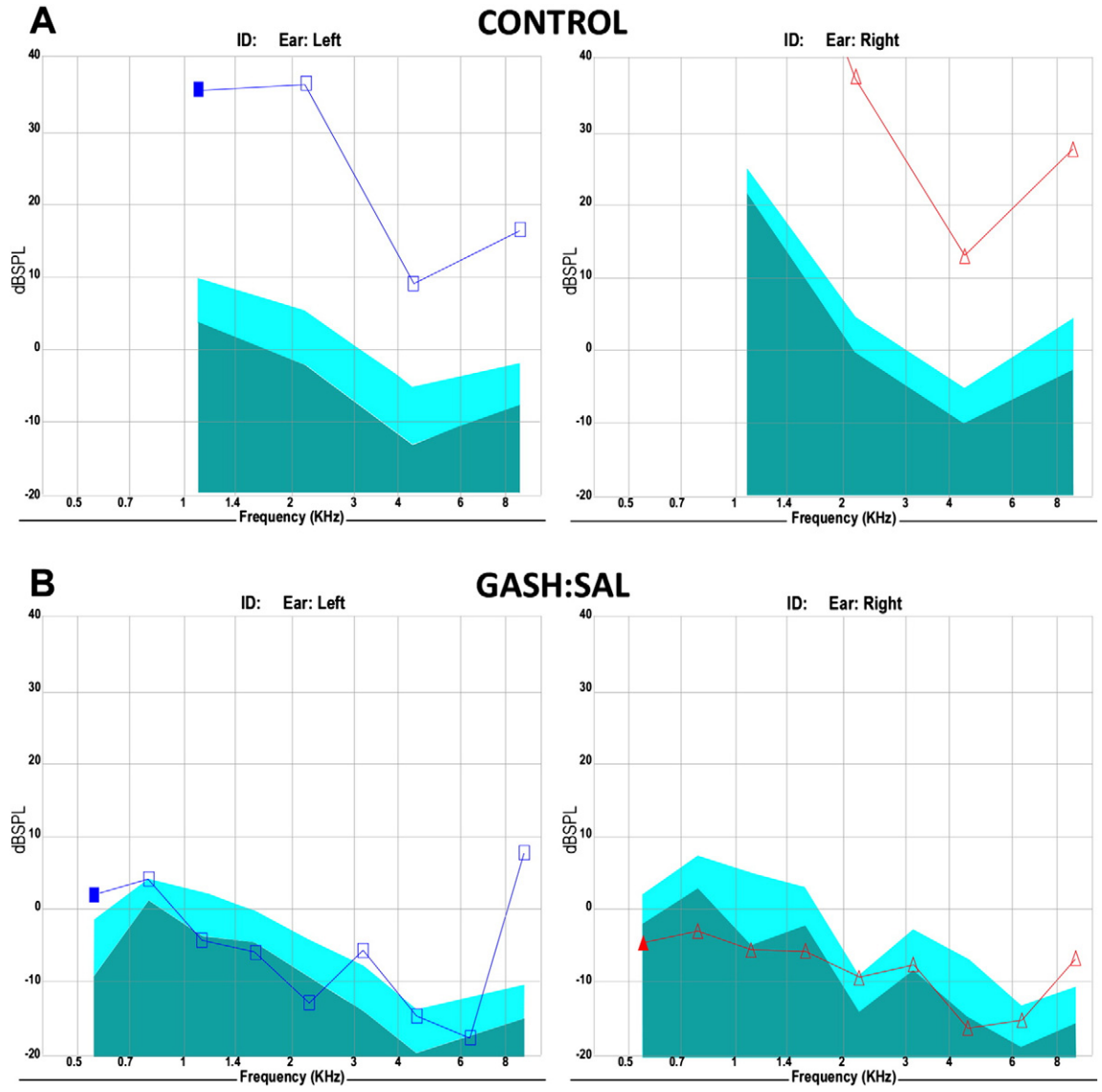

Fig. 3. Distortion-product of otoacoustic emissions (DPOAEs) in the left and right ears of the control and GASH:Sal hamsters. A. Histogram showing present and normal DPOAEs in the left and right ears from a control hamster. Both signal-to-noise ratio and absolute amplitude values are adequate and robust. B. Histogram showing a clearly absent DPOAEs in a GASH:Sal hamster. Notice that data points corresponding to the low–middle frequency range (from 500 to 6000 Hz) are embedded in the noise floor for both ears. Also, DPOAEs were significantly higher in the left than in the right ear at a frequency of 8000 Hz (p value ≤ 0.001). The DPOAEs are denoted with squares (blue line) and with triangles (red line) for the left and right ears, respectively.

turns, although several OHCs and IHCs showed distortion in their stereociliary pattern (Fig. 4D).

As shown in greater detail in Fig. 5, the scanning electron microcopy study indicated a distortion and disarrangement in the organization pattern, as well as an altered morphology of the stereocilia in the OHCs and IHCs of the GASH:Sal.

3.3. Morphology of the olivocochlear neurons in the GASH:Sal

The evaluation of cochlear structure in the scanning electron microscopy showed morphofunctional alterations of the OHCs and the IHCs in the GASH:Sal. Therefore, we further analyzed the olivocochlear efferent neurons that innervate the cochlear hair cells, in order to find whether there is any morphological deficit in olivocochlear neurons. To achieve this, we visualized the olivocochlear efferent neurons by injection of the retrograde tracer FG into the left cochlea of control and GASH:Sal hamsters. In both animals, these injections generated retrograde labeling in the VNTB and LSO, and no labeled neurons were observed in any other auditory nuclei (Figs. 6 and 7), indicating that the injection sites were restricted to the cochlea.

Within the VNTB, we found labeled neurons that were identified as MOC neurons. They were large and multipolar neurons that distributed preferentially through the mediorostral extent of the VNTB with a clear contralateral preference. Thus, 80% of MOC neurons were found in the VTNB contralateral to the injection site, and 20% were ipsilateral (Fig. 7). Within the LSO and its surroundings, we found retrogradely labeled neurons that fit into the category of intrinsic and extrinsic LOC neurons, respectively. Intrinsic LSO neurons had an ovoid, fusiform shape and exhibited two or three primary dendrites (Fig. 8). In contrast, shell neurons were larger with a polygonal, globular, or elongated cell body and two or more dendrites that coursed along the edges of the LSO (Fig. 8). Intrinsic and extrinsic LOC neurons distributed mainly in the caudomedial extent of the LSO with a clear ipsilateral preference. Approximately, 90% of LOC and shell neurons were predominantly found ipsilateral to the side of the injection site (Fig. 7). A comparison between the control and the GASH:Sal hamsters showed that there

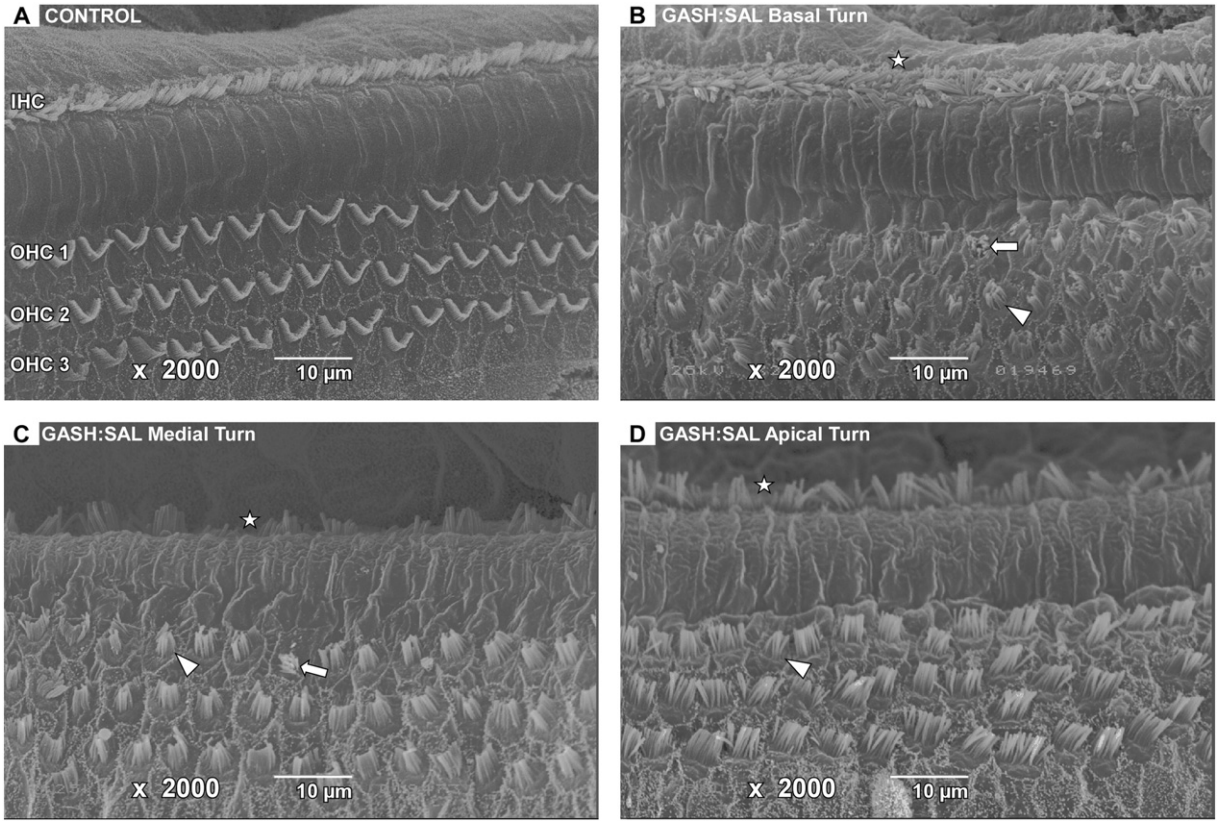

Fig. 4. Scanning electron microscopy of the organ of Corti in the control and GASH:Sal hamsters. A. Electron micrograph shows the organ of Corti in a control hamster. Notice normal distribution pattern of outer hair cells (OHCs) and inner hair cells (IHCs). Also, the stereocilia of the IHCs and OHCs exhibit the normal morphology, straight or slightly curved bundles for IHCs and V-shaped pattern for the three OHCs' rows (OHCs 1–3). B–D. Electron micrographs show the basal (B), medial (C), and apical (D) turns of the cochlea in the GASH:Sal. Notice the stereocilia distortion in the three rows of the OHCs and in the IHCs. Shortened stereocilia (arrows) as well as distortion and collapse of the stereociliary tufts (arrowheads) in the OHCs were frequently observed. V-like pattern of OHC stereocilia was absent in the corresponding three rows (OHCs 1–3). Stars indicate distortion of IHC stereocilia. Scale bars = 10 µm.

were no differences in the rostrocaudal distribution of MOC, LOC, and shell neurons (Fig. 7).

The difference in the number of intrinsic LOC and MOC neurons located ipsilateral vs. contralateral to the injected cochlea was statistically significant in control and GASH:Sal hamsters (p value ≤ 0.001, Table 1). Although we found fewer labeled neurons in the GASH:Sal than in the control hamster, this difference was not statistically significant (Fig. 9A and Table 1).

Regarding the size of the labeled olivocochlear neurons, we qualitatively observed that MOC, LOC, and shell neurons in the GASH:Sal had smaller cell bodies than that in the control hamster (Fig. 8).

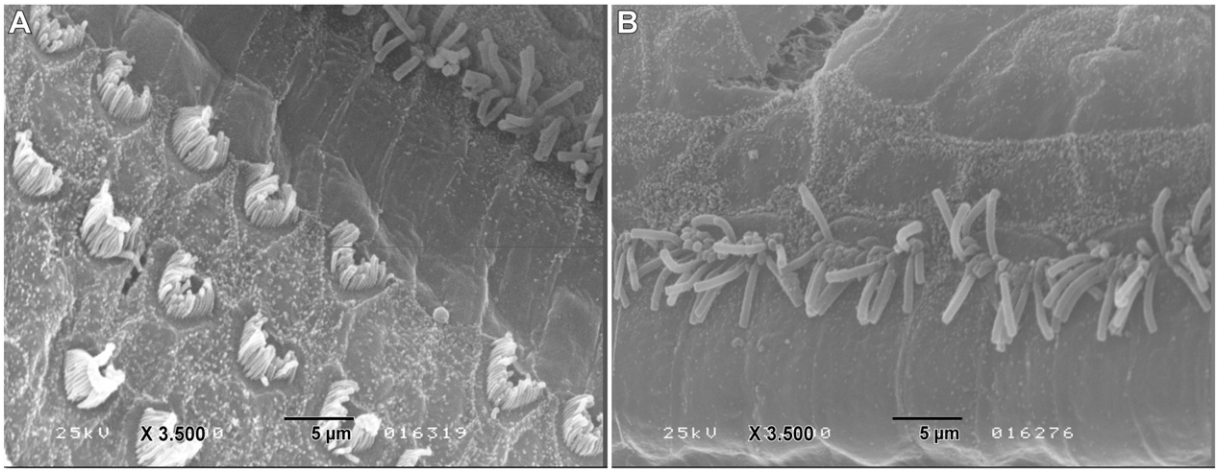

Fig. 5. Details of the stereocilia in the outer and inner hair cells (OHCs and IHCs) of the GASH:Sal. A. High magnification electron micrograph shows collapsed stereocilia in the OHCs. B. High magnification electron micrograph shows disrupted stereocilia pattern of the IHCs. Scale bars = 5 µm.

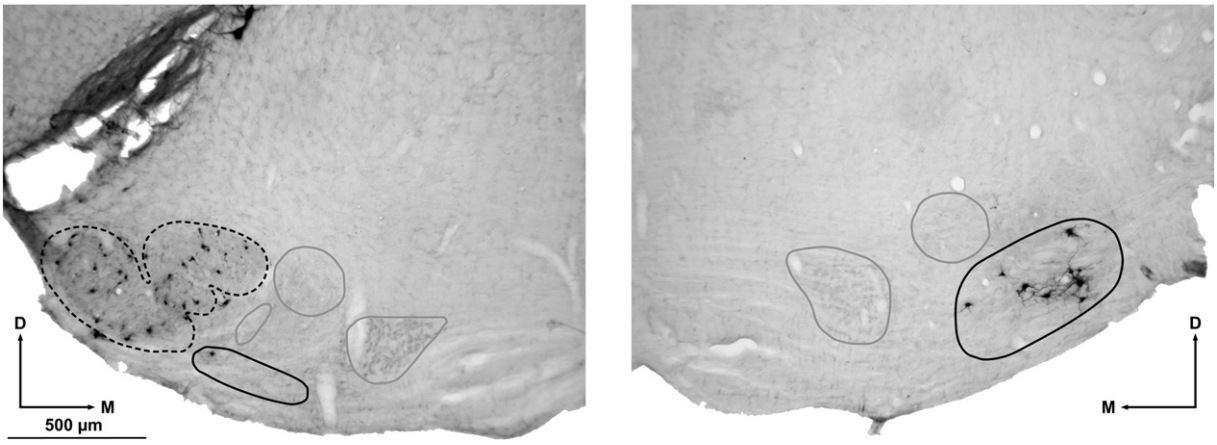

Fig. 6. Retrogradely labeled olivocochlear neurons after Fluoro-Gold injections into the left cochlea of the GASH:Sal. Micrographs show lateral olivocochlear (LOC) neurons in the ipsilateral lateral superior olive (LSO, denoted with dashed line) and medial olivocochlear (MOC) neurons in the contralateral ventral nucleus of the trapezoid body (VNTB, denoted with black solid line). Notice that no labeling was found in any other auditory nuclei (denoted in gray line). Scale bar = 500 μm.

The morphometric analysis of the soma areas of LOC and shell neurons located in the ipsilateral side to the injected cochlea confirmed that those neurons were significantly smaller in the GASH:Sal than in the control hamster (Fig. 9B and Table 2). Also, the soma areas of MOC neurons were significantly smaller in the GASH:Sal than in the control hamster (Fig. 9B and Table 2). When comparing the soma areas of LOC, MOC, and shell neurons depending on their ipsi- vs. contralateral location, we found that the sizes of the olivocochlear neurons were statistically different in the GASH:Sal (Fig. 9B and Table 2). In the GASH:Sal, soma areas of intrinsic and extrinsic LOC neurons were significantly smaller in the ipsilateral than in the contralateral side, and the soma areas of the MOC neurons were larger in the ipsilateral than in the contralateral side (Fig. 9B and Table 2). Such differences in soma areas were not found in the control animals with the exception of the shell neurons (Fig. 9B and Table 2).

Furthermore, we analyzed the roundness of the olivocochlear neurons in the control and GASH:Sal hamsters. There were no significant differences in the soma roundness between the control and GASH:Sal hamsters, except for the MOC neurons that were located on the side contralateral to the injection site. These neurons exhibited significantly more circular cell bodies in the GASH:Sal than in the control hamster (Fig. 9C).

3.4. 3D reconstruction of the LSO

The morphometric analyses indicated differences in the soma areas of the LOC neurons between the control and GASH:Sal hamsters. To verify whether these neuronal soma differences contributed to differences in the volume of the LSO, we performed a 3D reconstruction of the LSO in the control and GASH:Sal hamsters. The 3D reconstruction showed the characteristic S-like shape of the LSO (Fig. 10). When we compared control versus GASH:Sal hamsters, we found a statistically significant reduction in the volume of the LSO in the GASH:Sal. The LSO had a volume of 147,380,000 μm^3 in the control hamster, whereas the GASH:Sal hamster had a total volume of 104,790,000 μm^3 in the LSO (Fig. 10B). Therefore, our data showed a reduction in the LSO volume of almost 30% in the GASH:Sal. Such reduction in volume was also evident in the LSO area that was significantly reduced in the GASH:Sal. Our results showed that the LSO area was 1,973,300 μm^2 in the control hamster, while the LSO area in the GASH:Sal hamster was 1,411,655 μm^2 (Fig. 10C). Although there was no statistically significant difference in the total perimeter of the LSO between the control and GASH:Sal hamster (Fig. 10D), the LSO perimeter in each of the analyzed sections through the rostrocaudal extent of the nucleus was significantly smaller in the GASH:Sal than in the control.

4. Discussion

The present study showed functional and morphological alterations in the olivocochlear efferent system of the GASH:Sal. The ABR screening test indicated that the GASH:Sal exhibited asymmetric hearing alterations with higher ABR thresholds than controls. Also, the DPOAE analysis showed an absence of DPOAEs in the low–middle frequency range in both ears. These alterations in the olivocochlear efferent function of the GASH:Sal were associated with morphological alterations in the organ of Corti, size of the olivocochlear neurons, and volume of the LSO. Since the olivocochlear efferent system modulates the cochlear gain improving the auditory afferent information [29–31], its malfunctioning might be involved in the initiation and propagation of audiogenic seizures in the GASH:Sal.

4.1. Alterations in the peripheral auditory activity of the GASH:Sal

Recent studies from our research group have reported differences in ABR thresholds between the control and GASH:Sal hamsters [4]. In those experiments, the ABRs were assessed by acoustic stimulation in open field, showing ABR thresholds of approximately 40 dB and 80 dB for the control and GASH:Sal hamsters, respectively. In the present study, we have further assessed the ABR in the GASH:Sal by acoustic stimulation through inserted earphones. Our results showed that the ABR thresholds in the GASH:Sal were 50 dB and 60 dB after acoustic stimulation in the left and right ears, respectively. These ABR thresholds were lower than those obtained by Muñoz et al. [4], probably because of the different stimulation method. Despite this methodological difference, our results were in accordance with that study, showing higher ABR thresholds in the GASH:Sal than in the control hamsters. The ABR thresholds in young adult hamsters have been previously studied and were about 32 dB in response to click stimulation [32,33]. The ABR thresholds in the GASH:Sal were 50–60 dB, and hence, they were elevated by approximately 30 dB when compared with those in Syrian hamsters. Thus, our study confirmed hearing deficits and alterations in the auditory thresholds of the GASH:Sal. We also found differences in ABR latencies between the left and right ears of the GASH:Sal, showing higher ABR latencies for the left ear. This was verified by analyzing the interpeak latencies, which were significantly longer in duration for the waves III–V and I–V for the left ear compared with those for the right ear. Altogether, these data suggest a delay in the left auditory brainstem processing of the GASH:Sal. Such difference between the left and right auditory processing was not observed in the control hamster. In the GASH:Sal, we also found no differences between the right and left ears for the absolute latencies to I (auditory nerve) and II (cochlear nuclei)

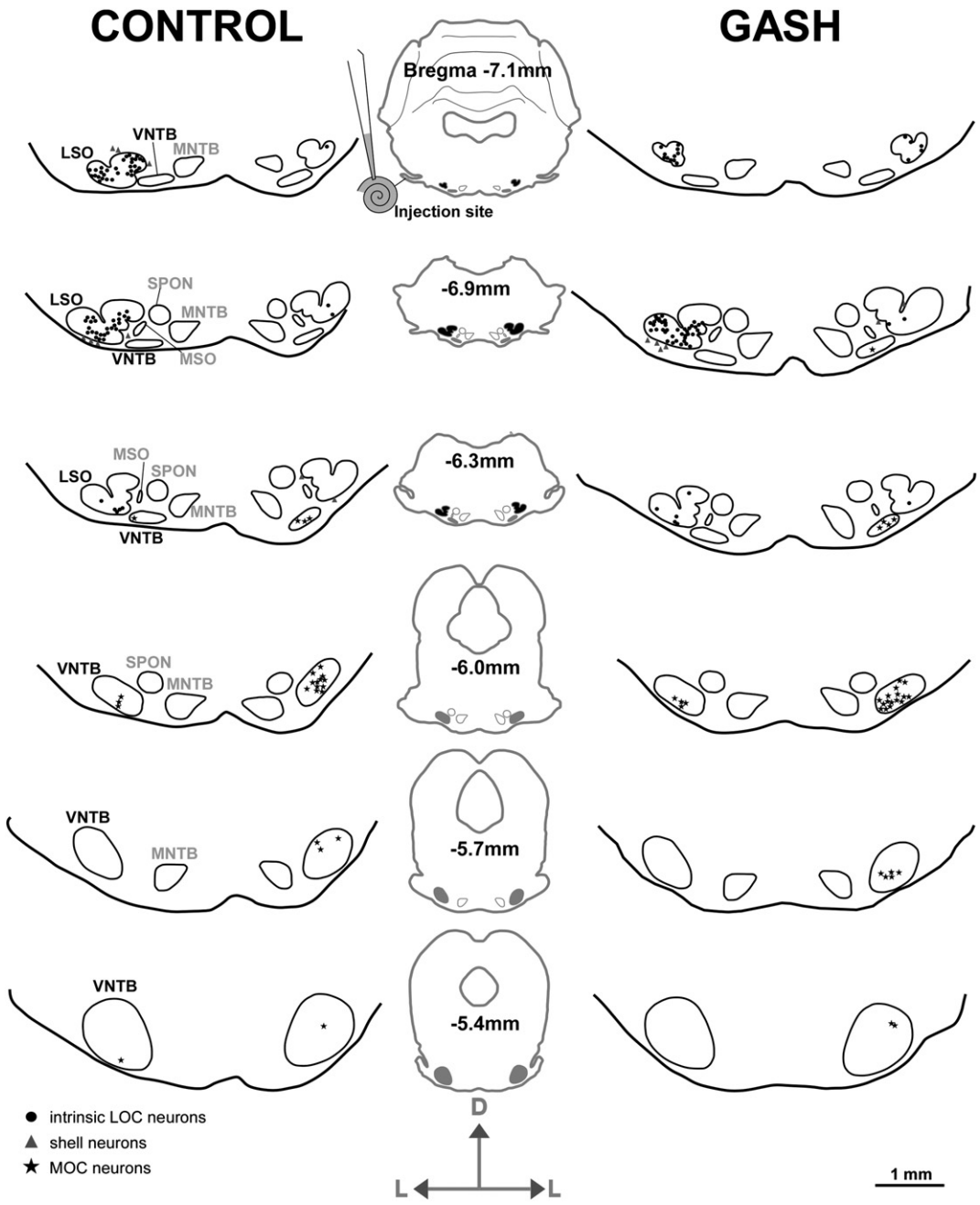

Fig. 7. Schematic drawings of coronal sections depicting the distribution of retrogradely labeled olivocochlear neurons after Fluoro-Gold injections into the left cochlea. Sections are arranged from caudal to rostral with distance relative to Bregma in mm. The center column shows the caudorostral distribution of the LSO (in black) and the VNTB (in gray). Notice the ipsi- vs. contraleral distribution of the lateral olivocochlear (LOC) and medial olivocochlear (MOC) neurons. LSO, lateral superior olive; MNTB, medial nucleus of the trapezoid body; MSO, medial superior olive; SPON, superior periolivary nucleus; VNTB, ventral nucleus of the trapezoid body. Symbols: circles = LOC neurons; triangles = shell neurons; stars = MOC neurons. Scale bar = 1 mm.

waves and interpeak symmetric latencies to ABR I–III waves. Thus, the auditory asymmetry in the auditory brainstem pathway occurs beyond the cochlear nucleus and includes the superior olivary complex (wave III), the inferior colliculus (wave IV), and the medial geniculate body (wave V). At the cochlear level of the GASH:Sal, we also reported differences between left and right ears, showing higher left-ear DPOAE amplitudes at a frequency of 8 kHz. Also, our study showed an absence of DPOAEs in the low–middle frequency range of the GASH:Sal, while the control hamsters showed normal presence of DPOAEs without left–right auditory asymmetry. Supporting this, previous studies in control mice reported no differences between left and right ears in DPOAE amplitudes at 8 kHz [34].

In humans, it is known that the right ear is more sensitive than the left to simple sounds, the so-called peripheral right-ear advantage that became manifested in higher otoacoustic emission amplitudes for the right ear compared with those for the left ear [35]. Thus, our DPOAE evaluation showed that the GASH:Sal exhibited, contrary to our expectations, a lateralization in auditory brainstem processing with a left side-ear dominance. This lateralization might be a distinct auditory feature of the GASH:Sal that has to be considered for future investigations related to seizures. In humans, electrophysiological lateralization of auditory evoked potentials has been found in patients with temporal lobe epilepsy, showing significant reduction in amplitude over the left hemisphere [36]. The auditory pathway ends at the temporal lobe, and

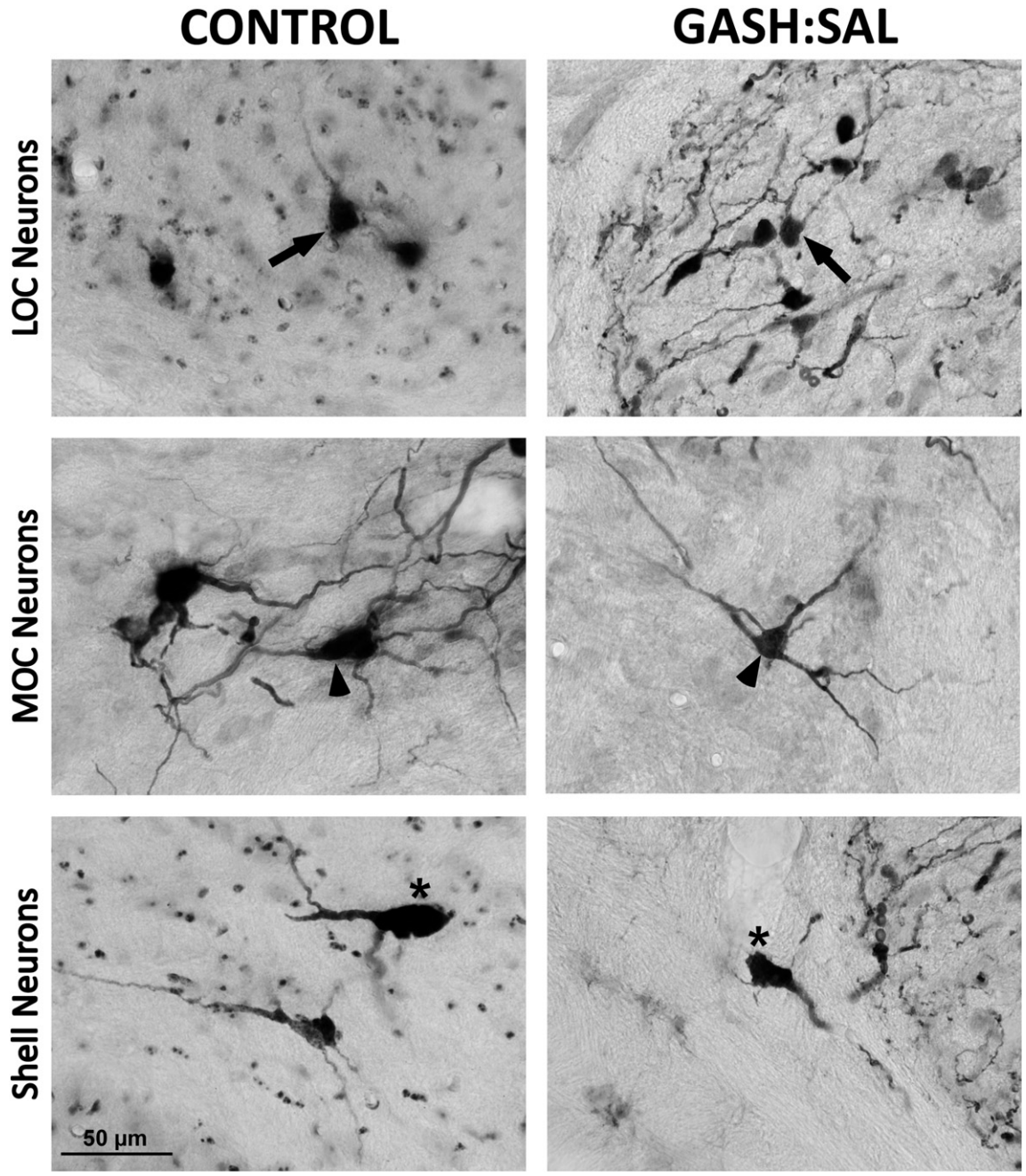

Fig. 8. Olivocochlear immunolabeled neurons after Fluoro-Gold injection into the left cochlea. LOC, MOC, and shell neurons are shown from upper to bottom panels, respectively. Notice that LOC neurons (denoted with arrows), MOC neurons (denoted with arrowheads), and shell neurons (denoted with asterisks) in the GASH:Sal (right panel) are smaller than in the control hamster (left panel). All microphotographs display the same magnification. Scale bar = 50 µm. MOC, medial olivocochlear; LOC, lateral olivocochlear.

Table 1
Average number and percentage of olivocochlear neurons labeled with Fluoro-Gold in the control and GASH:Sal hamsters. Notice the difference in percentage of olivocochlear neurons based on the ipsi- vs. contralateral location.

	Control		GASH:Sal	
	n	%	n	%
Ipsi LOC	369	59.97%	294.33	53.03%
Ipsi Shell	27.67	4.5%	21.67	3.9%
Ispi MOC	29.67	4.82%	45.67	8.23%
Contra LOC	44	7.15%	20.33	3.66%
Contra Shell	6	0.98%	3.33	0.6%
Contra MOC	139	22.59%	169.67	30.57%
Total	615.33	100	555	100

hence, patients with temporal lobe epilepsy had more deficits in auditory processing than those without cortical damage [37]. These asymmetrical hearing alterations are thought to be caused by the seizures that impair the anatomical and functional integrity of the auditory brainstem pathway [37]. Our ABR and DPOAE results indicated that the GASH:Sal also exhibited an asymmetrical hearing alteration, even though the GASH:Sal hamsters were naïve without having suffered epileptic seizures. Thus, our data suggest that the GASH:Sal has innate functional alterations in the olivocochlear efferent system that impair its auditory sensitivity, making it particularly susceptible to audiogenic seizures. The fact that we found an absence of DPOAEs in both ears is consistent with an altered medial olivocochlear function in the GASH:Sal. The medial olivocochlear system reduces the gain of the cochlear amplifier

through reflexive activation by sound, and the DPOAE test is used as an indicator of the status of the medial olivocochlear efferent system [31,38]. Since the GASH:Sal exhibited an absence of the DPOAEs, the medial olivocochlear efferent system is not able to turn down the cochlear response to sound, and as a result, this might contribute to trigger audiogenic seizures. However, it could be argued that the deficits observed in the ABRs and DPOAEs of the GASH:Sal were caused by the anesthetic. The anesthetic used in our study was ketamine–xylazine that produced an adequate level of anesthesia without tissue damage and has been commonly used in rodents to assess the integrity of the auditory brainstem, without alterations on ABRs or DPOAEs [39–41]. Furthermore, and more importantly, our study demonstrated changes in the anatomy of the olivocochlear efferent system, including the organ of Corti and olivocochlear neurons, which correlated with the alterations shown in the ABRs and DPOAEs of the GASH:Sal.

4.2. Morphological alterations in the olivocochlear efferent system of the GAH:Sal

One of the main goals of the present study was to determine whether the functional alterations observed in the peripheral auditory activity of the GASH:Sal have their corresponding anatomical correlations. A considerable number of studies used ABR and DPOAE tests to assess damage in the cochlea and in the brainstem auditory pathway, as well as an indicator of OHC function and the status of the olivocochlear efferent system [42–44]. To further explore our ABR and DPOAE results in the GASH:Sal, we performed a morphological study of the efferent olivocochlear system using a multi-technical approach that included a scanning electron microscopic analysis of the organ of Corti, a morphometric analysis of the olivocochlear neurons, and a 3D reconstruction of the LSO. At the cochlear level, our electron microscopy results showed that the stereociliary organization of the cochlear hair cells in the GASH:Sal was drastically impaired when compared with that in the control hamsters. The distorted pattern of the IHC stereocilia might correlate with high ABR thresholds observed in the GASH:Sal. Furthermore, the GASH:Sal exhibited deficits in the organization of the OHC stereocilia from basal to apical cochlear turns, which is consistent with the absence of DPOAEs over a wide frequency range. At the auditory brainstem level, the morphometric analysis of olivocochlear neurons in the GASH:Sal revealed a significant reduction in cell body size compared with that in the control hamsters. This morphometric analysis was carried out in retrogradely labeled neurons after injections of FG into the cochlea. Consistently with previous track-tracing studies in rodents [21,44,45], our injections generated retrograde labeling of the three types of olivocochlear neurons: LOC, MOC, and shell neurons. We also obtained a distribution pattern of olivocochlear neurons at the ipsicontralateral and rostrocaudal levels, in the GASH:Sal and control hamsters, which was similar to that reported in other rodents [21,46–49]. In our material, the total number of olivocochlear neurons in the control and GASH:Sal hamsters was higher than that obtained in our previous study using FG injections into the hamster's cochlea [21]. In fact, our quantification was very similar to that obtained in the mouse [47]. This rather unexpected result might be explained by the differences in the injection procedure that leads to different efficiencies in the neuronal tracer uptake. Despite this difference in the total number of labeled neurons, the percentage of labeled neurons in the LSO and VNTB was very similar in both studies (our results; [21]). Interestingly, one would expect to find a reduction in the number of MOC neurons in the GASH:Sal compared with that in the controls, based on the DPOAE alterations of the GASH:Sal. However, we observed a tendency towards a reduction in the number of labeled olivocochlear neurons in the GASH:Sal that was not statistically significant when compared with that in the controls. This might be explained because deficits in ABRs and DPOAEs do not necessarily involve degeneration of olivocochlear neurons. Supporting this argument, a recent study using ABR and DPOAE tests combined with FG injections in the cochlea indicated that, in acoustic trauma, LOC and MOC neurons remain intact despite hair cell dysfunction [44]. Our statistical comparative analysis of the soma area indicated that the MOC, LOC, and shell neurons of the ipsilateral side were significantly smaller in the GASH:Sal than in controls, as well as MOC neurons of the contralateral side. These results might be related to the asymmetrical hearing alteration found in our ABR and DPOAE results in the GASH:Sal. Although LOC and shell neurons of the contralateral side were also smaller in the GASH:Sal, we obtained no significant differences compared with those in controls. This lack of significant difference might be explained by the few LOC and shell neurons that were contralaterally labeled with FG, due to the fact that the lateral olivocochlear projection is predominantly ipsilateral [21]. To verify whether the neural size affected the size of the nucleus, we carried out a 3D reconstruction analysis of the LSO as a representative example. Our results confirmed that the area and volume of the LSO were significantly smaller in the GASH:Sal than in the control hamster. Supporting this, a previous study in other neuronal structures has also found that shrinkage of neurons contributes to the reduction of the nucleus' volume [50]. Further experiments are necessary to verify this reduction in the VNTB and to assess whether the differences in neuropil (dendrites and afferent and efferent axons) also contribute to the reduction of the LSO volume in the GASH:Sal. The LSO and VNTB send ascending inputs to the IC [51,52], which in turn, sends to a much lesser extent descending inputs to the LSO and VNTB [27,53]. Since the IC is a key structure in the initiation of audiogenic seizures [54–56], deficits in these reciprocal connections might contribute to the epileptogenesis in the IC of the GASH:Sal. Also, the descending olivocochlear pathway is influenced from higher auditory nuclei that adapt hearing function according to cortical analysis of the ascending auditory input [57]. Thus, alterations in the olivocochlear efferent system of the GASH:Sal might be due to malfunctioning of the feedback from higher auditory nuclei. One of the most intriguing questions regarding the epileptogenic process in the GASH:Sal is whether the seizures induced the morphological changes in the auditory system or, conversely, morphological alterations underlie the susceptibility of the GASH:Sal to audiogenic seizure. In our study, the GASH:Sal animals were nonstimulated and did not suffer any epileptic seizure. Therefore, the morphological alterations of the olivocochlear efferent system in the GASH:Sal are innate components of this animal model, and hence, it can be inferred that such alterations have genetic origin. The audiogenic seizure pathology in the GASH:Sal model is a form of reflex epilepsy, manifested as generalized tonic–clonic seizures after external acoustic stimulation [1,3,5]. In humans, the pathogenesis underlying acoustic reflex epilepsies is not clear, whether the seizure susceptibility originates in the central or peripheral auditory system. Our study provides important information with this respect and supports the GASH:Sal as a valuable animal model to investigate the links between the morphological alterations and the seizures, as well as for better understanding the cause of acoustic hypersensitivity.

5. Conclusions

The olivocochlear efferent system of the GASH:Sal has functional and morphological alterations. The GASH:Sal exhibited high ABR thresholds as well as an absence of DPOAEs in a wide range of frequencies and a clear lateralization in auditory brainstem processing. Since this left–right auditory asymmetry was not present in control hamsters, it might be a distinct auditory feature of the GASH:Sal.

Morphological alterations in the olivocochlear efferent system of the GASH:Sal were observed from the cochlear receptor to the SOC. At the cochlear level, there is a derangement and distortion of the cochlear stereocilia from basal to apical cochlear turns of the GASH:Sal that were not observed in the control hamster. At the brainstem level, the olivocochlear neurons, including MOC, LOC, and shell

neurons, have reduced soma areas compared with those of control animals. This neuron shrinkage contributes to the reduction of the LSO volume as shown in the 3D reconstruction analysis. The functional alterations of the peripheral auditory activity were positively correlated with the morphological alterations of the olivocochlear efferent system.

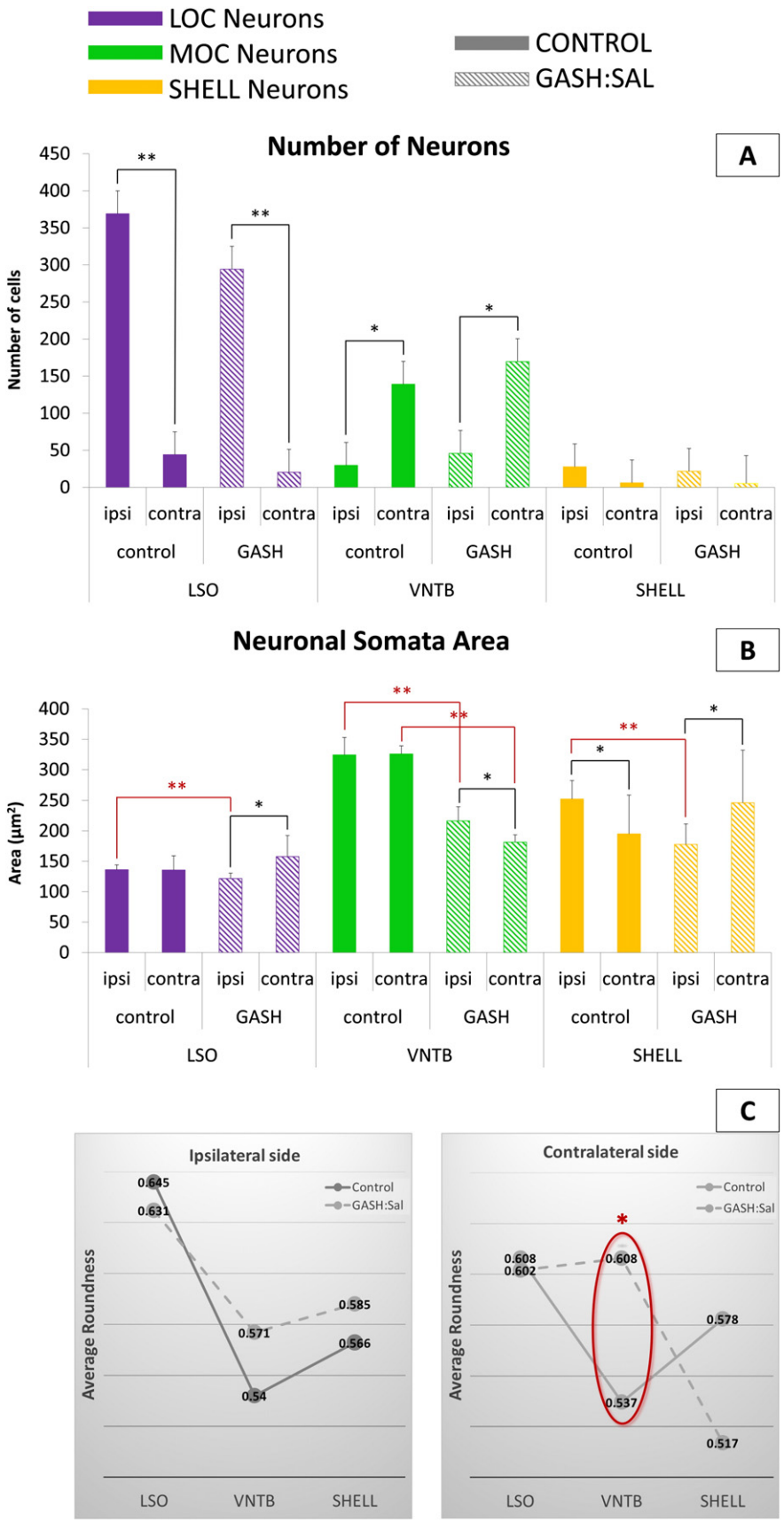

Table 2
Neuronal somata areas (in μm^2) of the three types of olivocochlear neurons (LOC, MOC, shell) in control and GASH:Sal hamsters.

	LOC		MOC		Shell	
	Ipsi-	Contra-	Ipsi-	Contra-	Ipsi-	Contra-
Control	136,079	135,476	324.21	325.78	252,354	195,112
GASH:Sal	121.632**	157,711	216.366**	181.588**	177.801**	246,367

** Significant difference with respect to control p value < 0.01.

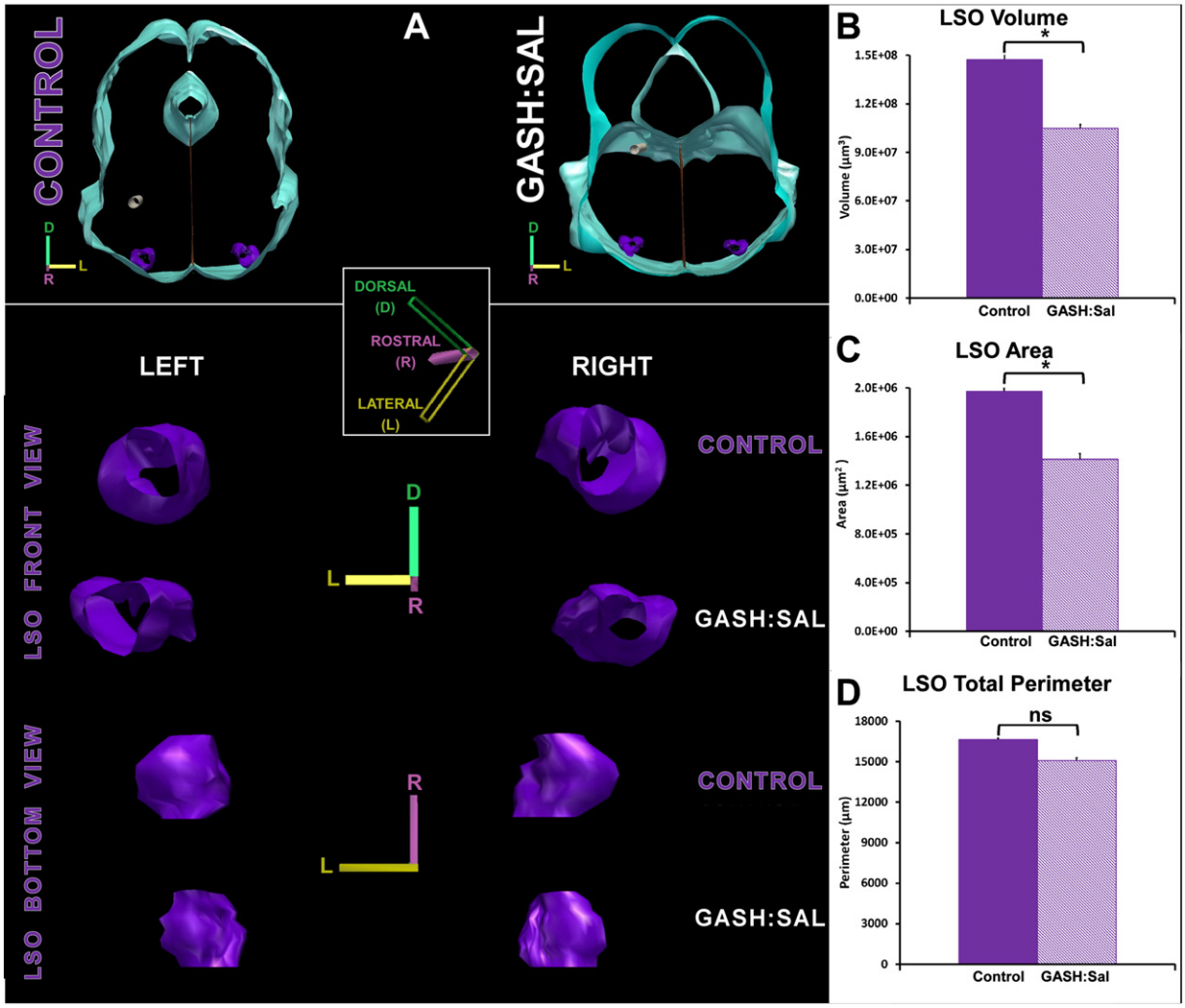

Fig. 10. Differences in the size of the lateral superior olive (LSO) between the control and GASH:Sal hamsters. A. 3D reconstruction of the LSO in the control and GASH:Sal hamsters. The upper panel shows the reconstruction of brainstem sections in which the LSO was found. The lower panel shows different views of the 3D reconstruction (front and bottom views) in the control and GASH:Sal hamsters. Each scale bar represents 500 µm. B–D. Histograms show the LSO volume (B), area (C), and perimeter (D) in the control and GASH:Sal hamsters. "*" = p value ≤ 0.05; ns = nonsignificant.

The functional and morphological alterations in the olivocochlear efferent system are intrinsic and innate components of the GASH:Sal and might impair its auditory sensitivity, making them particularly susceptible to audiogenic seizures.

Acknowledgments

This study was supported by the Spanish JCyL (#SA023A12-2), the University of Salamanca Research grant to (GIR 2016-184092), and

Fig. 9. Morphometric analysis of the labeled olivocochlear neurons after Fluoro-Gold injection into the left cochlea. A. Histogram shows the number of olivocochlear neurons in the ipsi- and contralateral sides of control and GASH:Sal hamsters. B. Histogram shows the neuronal soma areas in the ipsi- and contralateral sides of control and GASH:Sal hamsters. For histograms A and B, LOC neurons are displayed in purple, MOC neurons in green, and shell neurons in yellow. Solid histogram bars are used for control hamsters and striped histogram bars for GASH:Sal. "*" = p value ≤ 0.05 and "**" = p value ≤ 0.01. Black lines have been used for comparison between ipsi- and contralateral sides whereas red lines have been used for comparison between control and GASH:Sal hamsters. C. Plots show the soma roundness of olivocochlear neurons in the ipsi- (left plot) and contralateral sides (right plot) of control (solid line) and GASH:Sal (dashed line) hamsters. Notice that the roundness of MOC neurons of the VNTB was significantly different between the control and GASH:Sal hamsters (red oval). "*" = p value ≤ 0.05. LOC, lateral olivocochlear; LSO, lateral superior olive; MOC, medial olivocochlear; VNTB, ventral nucleus of the trapezoid body.

the University of São Paulo (USP)/University of Salamanca (USAL) Program for the Promotion of the Bilateral Cooperation in the Field of Research (#2011.1.23386.1.3; #2011.1.23386.1.3). Other financial support: FAPESP (#2007/50261-4), FAPESP-Cinapce (#2005/56447-7), CNPq, and CAPES-PROEX.

Conflict of interest

The authors certify that they have no affiliations with or involvement in any organization or entity with any financial interest (such as honoraria, educational grants, participation in speakers' bureaus, membership, employment, consultancies, stock ownership, or other equity interest or expert testimony or patent-licensing arrangements) or non-financial interest (such as personal or professional relationships, affiliations, knowledge, or beliefs) in the subject matter or materials discussed in this manuscript.

References

[1] Muñoz de la Pascua L, López-García DE. In: Muñoz L, editor. Establecimiento y caracterización de una línea de hámsters sirios propensos a padecer convulsiones audiógenas; 2004 [ISBN 13: 978-84-609-5027-1].
[2] Prieto-Martín AI, Llorens S, Pardal-Fernández JM, Muñoz LJ, López DE, Escribano J, et al. Opposite caudal versus rostral brain nitric oxide synthase response to generalized seizures in a novel rodent model of reflex epilepsy. Life Sci 2012;90(13–14):531–7.
[3] Carballosa-Gonzalez MM, Muñoz LJ, López-Alburquerque T, Pardal-Fernández JM, Nava E, de Cabo C, et al. EEG characterization of audiogenic seizures in the hamster strain GASH:Sal. Epilepsy Res 2013;106(3):318–25.
[4] Muñoz LJ, Carballosa-Gautam MM, Yanowsky K, Garcia-Atarés N, López DE. The genetic audiogenic seizure hamster from Salamanca: The GASH:Sal. Epilepsy Behav 2017;71:181–92.
[5] Barrera-Bailón B, Oliveira JA, López DE, Muñoz LJ, Garcia-Cairasco N, Sancho C. Pharmacological and neuroethological studies of three antiepileptic drugs in the genetic audiogenic seizure hamster (GASH:Sal). Epilepsy Behav 2013;28(3):413–25.
[6] Sancho C, Barrera-Bailón B, Oliveira JAC, López DE, Muñoz LJ, Garcia-Cairasco N. Pharmacological validation of the genetic audiogenic seizure hamster (GASH:Sal) using several antiepileptics. Epilepsy Behav 2013;28(3):413–25.
[7] Faingold CL. The role of the brain stem in generalized epileptic seizures. Metab Brain Dis 1987;2(2):81–112.
[8] Moraes MF, Garcia-Cairasco N. Real time mapping of rat midbrain neural circuitry using auditory evoked potentials. Hear Res 2001;161(1–2):35–44.
[9] Kandratavicius L, Balista PA, Lopes-Aguiar C, Ruggiero RN, Umeoka EH, Garcia-Cairasco N, et al. Animal models of epilepsy: use and limitations. Neuropsychiatr Dis Treat 2014;10:1693–705.
[10] Racine RJ. Modification of seizure activity by electrical stimulation. Electroencephalogr Clin Neurophysiol 1972;32:281–7.
[11] Garcia-Cairasco N, Terra VC, Doretto MC. Midbrain substrates of audiogenic seizures in rats. Behav Brain Res 1993;58(1–2):57–67.
[12] Garcia-Cairasco N, Doretto MC, Ramalho MJ, Antunes-Rodrigues J, Nonaka KO. Audiogenic and audiogenic-like seizures: locus of induction and seizure severity determine postictal prolactin patterns. Pharmacol Biochem Behav 1996;53(3):503–10.
[13] Faingold CL. Neuronal networks in the genetically epilepsy-prone rat. Adv Neurol 1999;79:311–21.
[14] Warr WB. Organization of olivocochlear efferent systems in mammals. In: Webster DB, Popper AN, Fay RR, editors. The mammalian auditory pathway: neuroanatomy. New York: Springer; 1992. p. 410–48.
[15] Mulders WH, Robertson D. Morphological relationships of peptidergic and noradrenergic nerve terminals to olivocochlear neurons in the rat. Hear Res 2000;144(1–2):53–64.
[16] Xiao Z, Suga N. Modulation of cochlear hair cells by the auditory cortex in the mustached bat. Nat Neurosci 2002;5(1):57–63.
[17] Mulders WH, Robertson D. Effects on cochlear responses of activation of descending pathways from the inferior colliculus. Hear Res 2000;149(1–2):11–23.
[18] Dewson JH. Efferent olivocochlear bundle: some relationships to stimulus discrimination in noise. J Neurophysiol 1968;31:122–30.
[19] Oatman LC, Anderson BW. Effects of visual attention on tone burst evoked auditory potentials. Exp Neurol 1977;57:200–11.
[20] Scharf B, Magnan J, Chays A. On the role of the olivocochlear bundle in hearing: 16 case studies. Hear Res 1997;103(1–2):101–22.
[21] Sánchez-González MA, Warr WB, López DE. Anatomy of olivocochlear neurons in the hamster studied with FluoroGold. Hear Res 2003;185(1–2):65–76.
[22] Guinan Jr JJ. Physiology of olivocochlear efferents. In: Dallos P, Popper AN, Fay RR, editors. The cochlea. New York: Springer; 1996. p. 435–502.
[23] Le Prell CG, Bledsoe Jr SC, Bobbin RP, Puel JL. Neurotransmission in the inner ear: functional and molecular analysis. In: Santos-Sacchi J, Jahn AF, editors. Physiology of the ear. New York: Singular Publishing; 2001. p. 575–611.
[24] Glowatzki E, Fuchs PA. Cholinergic synaptic inhibition of inner hair cells in the neonatal mammalian cochlea. Science 2000;288(5475):2366–8.
[25] Puel JL, Ruel J, Guitton M, Wang J, Pujol R. The inner hair cell synaptic complex: physiology, pharmacology and new therapeutic strategies. Audiol Neurootol 2002;7(1):49–54.
[26] De Freitas MR, Figueiredo AA, Brito GA, Leitao RF, Carvalho Junior JV, Gomes Junior RM, et al. The role of apoptosis in cisplatin-induced ototoxicity in rats. Braz J Otorhinolaryngol 2009;75(5):745–52.
[27] Gómez-Nieto R, Rubio ME, López DE. Cholinergic input from the ventral nucleus of the trapezoid body to cochlear root neurons in rats. J Comp Neurol 2008;506(3):452–68.
[28] Hormigo S, Gómez-Nieto R, Castellano O, Herrero-Turrión MJ, López DE, de Anchieta de Castro e Horta-Júnior J. The noradrenergic projection from the locus coeruleus to the cochlear root neurons in rats. Brain Struct Funct 2015;220(3):1477–96.
[29] Warr WB, Guinan Jr JJ. Efferent innervation of the organ of corti: two separate systems. Brain Res Sep 7 1979;173(1):152–5.
[30] Liberman MC, Puria S, Guinan Jr JJ. The ipsilaterally evoked olivocochlear reflex causes rapid adaptation of the 2f1–f2 distortion product otoacoustic emission. J Acoust Soc Am 1996;99(6):3572–84.
[31] Puria S, Guinan Jr JJ, Liberman MC. Olivocochlear reflex assays: effects of contralateral sound on compound action potentials versus ear-canal distortion products. J Acoust Soc Am 1996;99(1):500–7.
[32] Church MW, Kaltenbach JA. The hamster's auditory brain stem response as a function of stimulus intensity, tone burst frequency, and hearing loss. Ear Hear 1993;14(4):249–57.
[33] Heffner HE, Harrington IA. Tinnitus in hamsters following exposure to intense sound. Hear Res 2002;170(1–2):83–95.
[34] Larsen E, Liberman MC. Contralateral cochlear effects of ipsilateral damage: no evidence for interaural coupling. Hear Res 2010;260(1–2):70–80.
[35] Khalfa S, Collet L. Functional asymmetry of medial olivocochlear system in humans. Towards a peripheral auditory lateralization. Neuroreport 1996;7(5):993–6.
[36] Brodtkorb E, Steinlein OK, Sand T. Asymmetry of long-latency auditory evoked potentials in LGI1-related autosomal dominant lateral temporal lobe epilepsy. Epilepsia 2005;46(10):1692–4.
[37] Meneguello J, Leonhardt FD, Pereira LD. Auditory processing in patients with temporal lobe epilepsy. Braz J Otorhinolaryngol 2006;72(4):496–504.
[38] Cooper NP, Guinan Jr JJ. Efferent-mediated control of basilar membrane motion. J Physiol 2006;576(Pt 1):49–54.
[39] Payton AJ, Forsythe DB, Dixon D, Myers PH, Clark JA, Snipe JR. Evaluation of ketamine–xylazine in Syrian hamsters. Cornell Vet 1993;83(2):153–61.
[40] Coomber B, Berger JI, Kowalkowski VL, Shackleton TM, Palmer AR, Wallace MN. Neural changes accompanying tinnitus following unilateral acoustic trauma in the guinea pig. Eur J Neurosci 2014;40(2):2427–41.
[41] Ruebhausen MR, Brozoski TJ, Bauer CA. A comparison of the effects of isoflurane and ketamine anesthesia on auditory brainstem response (ABR) thresholds in rats. Hear Res 2012;287(1–2):25–9.
[42] Izquierdo MA, Gutierrez-Conde PM, Merchan MA, Malmierca MS. Non-plastic reorganization of frequency coding in the inferior colliculus of the rat following noise-induced hearing loss. Neuroscience 2008;154:355–69.
[43] Charizopoulou N, Lelli A, Schraders M, Ray K, Hildebrand MS, Ramesh A, et al. Gipc3 mutations associated with audiogenic seizures and sensorineural hearing loss in mouse and human. Nat Commun 2011;2:201.
[44] Reuss S, Closhen C, Riemann R, Jaumann M, Knipper M, Rüttiger L. Absence of early neuronal death in the olivocochlear system following acoustic overstimulation. Anat Rec (Hoboken) 2016;299(1):103–10.
[45] Vetter DE, Mugnaini E. Distribution and dendritic features of three groups of rat olivocochlear neurons. A study with two retrograde cholera toxin tracers. Anat Embryol (Berl) 1992;185(1):1–16.
[46] White JS, Warr WB. The dual origins of the olivocochlear bundle in the albino rat. J Comp Neurol 1983;219(2):203–14.
[47] Campbell JP, Henson MM. Olivocochlear neurons in the brainstem of the mouse. Hear Res 1988;35(2–3):271–4.
[48] Warr WB, Boche JB, Neely ST. Efferent innervation of the inner hair cell region: origins and terminations of two lateral olivocochlear systems. Hear Res 1997;108(1–2):89–111.
[49] Brown MC, Levine JL. Dendrites of medial olivocochlear neurons in mouse. Neuroscience 2008;154(1):147–59.
[50] Loftus M, Knight RT, Amaral DG. An analysis of atrophy in the medial mammillary nucleus following hippocampal and fornix lesions in humans and nonhuman primates. Exp Neurol 2000;163(1):180–90.
[51] Oliver DL. Ascending efferent projections of the superior olivary complex. Microsc Res Tech 2000;51(4):355–63.
[52] Warr WB, Beck JE. Multiple projections from the ventral nucleus of the trapezoid body in the rat. Hear Res 1996;93(1–2):83–101.
[53] Faye-Lund H. Projection from the inferior colliculus to the superior olivary complex in the albino rat. Anat Embryol (Berl) 1986;175(1):35–52.
[54] Garcia-Cairasco N, Sabbatini RM. Possible interaction between the inferior colliculus and the substantia nigra in audiogenic seizures in Wistar rats. Physiol Behav 1991;50(2):421–7.
[55] Kesner RP. Subcortical mechanisms of audiogenic seizures. Exp Neurol 1966;15(2):192–205.
[56] Wada JA, Terao A, Scholtmeyer H, Trapp WG. Reversible audiogenic seizure susceptibility induced by hyperbaric oxygenation. Exp Neurol 1970;29(3):400–4.
[57] Khalfa S, Bougeard R, Morand N, Veuillet E, Isnard J, Guenot M, et al. Evidence of peripheral auditory activity modulation by the auditory cortex in humans. Neuroscience 2001;104(2):347–58.